UNIVERSITY of BRADFORD

Library

The University of Bradford Institutional Repository

http://bradscholars.brad.ac.uk

This work is made available online in accordance with publisher policies. Please refer to the repository record for this item and our Policy Document available from the repository home page for further information.

To see the final version of this work please visit the publisher's website. Access to the published online version may require a subscription.

Link to publisher's version: *http://dx.doi.org/10.1016/j.apenergy.2014.08.086*

Citation: Abeykoon C, Kelly AL, Vera-Sorroche J et al (2014) Process efficiency in polymer extrusion: Correlation between the energy demand and melt thermal stability. Applied Energy. 135: 560-571.

Copyright statement: © 2014 The Authors. This is an Open Access article licensed under the Creative Commons *CC-BY license*.

Applied Energy 135 (2014) 560–571

Contents lists available at ScienceDirect

Applied Energy

journal homepage: www.elsevier.com/locate/apenergy

Process efficiency in polymer extrusion: Correlation between the energy demand and melt thermal stability

Chamil Abeykoon [a,*], Adrian L. Kelly [a], Javier Vera-Sorroche [a], Elaine C. Brown [a], Phil D. Coates [a], Jing Deng [b], Kang Li [b], Eileen Harkin-Jones [c], Mark Price [c]

[a] IRC in Polymer Science and Technology, School of Engineering, Design and Technology, University of Bradford, Bradford BD7 1DP, UK
[b] School of Electronics, Electrical Engineering and Computer Science, Queen's University Belfast, Belfast BT9 5AH, UK
[c] School of Mechanical and Aerospace Engineering, Queen's University Belfast, Belfast BT9 5AH, UK

HIGHLIGHTS

- This paper discusses the energy conservation of an extruder.
- This describes the energy and thermal efficiencies in polymer extrusion.
- This explores the correlation between energy demand and thermal stability.
- This explores radial temperature fluctuations of the melt flow in extrusion.
- This models the total power demand in polymer extrusion empirically.

ARTICLE INFO

Article history:
Received 28 May 2013
Received in revised form 11 August 2014
Accepted 25 August 2014
Available online 25 September 2014

Keywords:
Polymer extrusion
Process monitoring
Melt viscosity
Energy demand
Thermal stability
Energy efficiency

ABSTRACT

Thermal stability is of major importance in polymer extrusion, where product quality is dependent upon the level of melt homogeneity achieved by the extruder screw. Extrusion is an energy intensive process and optimisation of process energy usage while maintaining melt stability is necessary in order to produce good quality product at low unit cost. Optimisation of process energy usage is timely as world energy prices have increased rapidly over the last few years. In the first part of this study, a general discussion was made on the efficiency of an extruder. Then, an attempt was made to explore correlations between melt thermal stability and energy demand in polymer extrusion under different process settings and screw geometries. A commodity grade of polystyrene was extruded using a highly instrumented single screw extruder, equipped with energy consumption and melt temperature field measurement. Moreover, the melt viscosity of the experimental material was observed by using an off-line rheometer. Results showed that specific energy demand of the extruder (i.e. energy for processing of unit mass of polymer) decreased with increasing throughput whilst fluctuation in energy demand also reduced. However, the relationship between melt temperature and extruder throughput was found to be complex, with temperature varying with radial position across the melt flow. Moreover, the melt thermal stability deteriorated as throughput was increased, meaning that a greater efficiency was achieved at the detriment of melt consistency. Extruder screw design also had a significant effect on the relationship between energy consumption and melt consistency. Overall, the relationship between the process energy demand and thermal stability seemed to be negatively correlated and also it was shown to be highly complex in nature. Moreover, the level of process understanding achieved here can help to inform selection of equipment and setting of operating conditions to optimise both energy and thermal efficiencies in parallel.
© 2014 The Authors. Published by Elsevier Ltd. This is an open access article under the CC BY license (http://creativecommons.org/licenses/by/3.0/).

1. Introduction

Polymeric materials are widely used all over the world primarily due to their superior properties such as high strength to weight ratio; high temperature/chemical/corrosive resistance; non-conductivity; high clarity; re-processability; low cost and so forth.

* Corresponding author.
E-mail addresses: Y.Aabeykoon@bradford.ac.uk, yabeykoon01@qub.ac.uk (C. Abeykoon), A.L.Kelly@bradford.ac.uk (A.L. Kelly).

http://dx.doi.org/10.1016/j.apenergy.2014.08.086
0306-2619/© 2014 The Authors. Published by Elsevier Ltd.
This is an open access article under the CC BY license (http://creativecommons.org/licenses/by/3.0/).

Nomenclature

a	the shift factor
C_1, C_2, T_s	empirical constants
C_p	the specific heat capacity of the material
$\overline{C}_p$	the average specific heat capacity of the polymer
D	diameter of the screw
E_{in}	the total energy supplied to the extruder
E_{losses}	the total amount of energy wasted without involving in any useful work
E_T	the theoretical energy required for melting and forming of material
E_u	the energy used for useful work
h_1	the specific enthalpy of the materials at the input
h_2	the specific enthalpy of the materials at the output
H_f	the enthalpy of heat of fusion of the materials
Δh	the changes of the enthalpy
$\dot{M}$	the mass flow rate
n	the power law index
P_1	the pressure at the input
P_2	the pressure at the output
T_1	the feedstock temperature at the input
T_2	the feedstock temperature at the output
T_r	a reference temperature
T_{mean}	the mean temperature across the melt flow
$f(T)$	the temperature function
T-IR	the temperature measured by the IR temperature sensor
$Trp-x, x = 0, 2.5, 5.0, 8.0, 11.0, 14.0, 16.5$	temperature of the melt at x mm away from the melt flow centreline (rp refers to radial position)
ΔT	the level of the melt temperature fluctuations across the melt flow
$\eta_{extruder}$	the extruder energy efficiency
ρ	the density of the material
$\bar{\rho}$	the average density of the material
$\eta_{extruder,thermo}$	the thermal efficiency of an extruder
μ	the viscosity
μ_0	the viscosity at zero shear rate
γ	the shear rate
λ	the relaxation time
ω_{sc}	screw speed

More importantly, polymeric materials are showing a great potential of saving energy consumption in aerospace, automotive, marine and transport sector. Moreover, they are quite easy to form into complex shapes compared to other conventional materials. Also, the energy requirement for processing of polymers is considerably lower than other conventional materials such as steel and glass. Perhaps, these may be among the major reasons for growing popularity of polymeric materials in diverse industrial sectors. Although the processing of polymers demands a less amount of energy compared to other materials [1], many polymer processes operate at poor energy efficiency. Usually, the specific energy consumption (SEC) in polymer extrusion reduces as processing speed increases [2,3]. However, the thermal fluctuations of the melt flow are increased as the process speed is increased [4–9]. Therefore, the majority of polymer processes are run at conservative rates to avoid thermal fluctuations at higher processing speeds. Currently, the polymer sector is under pressure to cut down excessive use of energy due to the gradual increase of energy prices in the world over the last few decades [10].

Usually, polymer extrusion is an unpredictable process and hence it is highly prone to fluctuations in nature. Moreover, the process parameters are complexly coupled each to other and hence difficult to set-up and control [7]. Therefore, the typical relationship between process thermal stability and energy efficiency may differ depending on the processing conditions; material and machine being used while the quality of the process monitoring and control also may have considerable effects. Among the polymer processing extruders, single screw continuous extruders are the most commonly used in industry [11] and that is mainly due to their low purchase and maintenance costs, simplicity of operation and the ability to generate the required pressure [12]. Therefore, this study is focused on single screw extrusion processes. More details on the process mechanisms, operational requirements, and the available process analytical techniques (PAT) of polymer extrusion can be found in the literature [13–16].

1.1. Efficiency of an extruder

An illustration of an extruder based on its energy conservation can be illustrated as shown in Fig. 1.

Then the energy used for useful work (E_u) from an extruder (i.e. the energy used for material melting and forming through the die) can be given as:

$$E_u = E_{in} - E_{losses} \tag{1}$$

where E_{in} is the total energy supplied to the extruder and E_{losses} is the total amount of energy wasted without involving in any useful work. Therefore, the extruder energy efficiency ($\eta_{extruder}$) is given by:

$$\eta_{extruder} = \frac{E_{in} - E_{losses}}{E_{in}} \times 100\% \tag{2}$$

Here, the energy inputs (E_{in}) are from the electrical energy supplied to the devices such as drive motor, motor cooling fan, barrel/die haters, barrel cooling fans, instruments in the control panel, and water pump. The energy losses which may occur in these devices and other mechanical/functional systems such as transmission, forced/natural cooling come under E_{losses}. Of the energy consuming devices, drive motor and barrel/die heaters are likely to consume more than 90% of the total energy supply while these are also responsible for the highest energy losses. In extrusion there is a little potential of useful recovery of rejected energy as these are largely released to air or water. Drury [17] argues that over 40% from the energy input to the small scale extruder is wasted through drive/transmission losses, radiation, convection, conduction losses, etc.

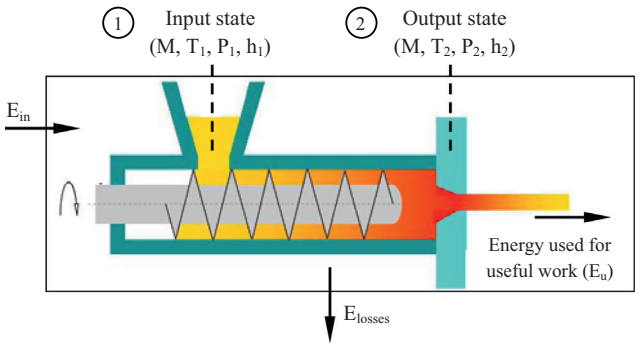

Fig. 1. An illustration of an extruder based on its energy.

The thermodynamic efficiency of an extruder can be determined by comparing the actual energy consumed by the extruder to the theoretical energy required to transform the polymer from initial (input) stage to the desired/output stage. Usually, the thermodynamic efficiency is calculated under the following assumptions:

- The extruder is under steady state operation.
- The process operates in uniform temperature, pressure and mass flow rate.
- The feed material entering to the extruder is assumed to be under uniform temperature and pressure.

The theoretical energy required for melting and forming (E_T) of material in polymer extrusion [18] is:

For semi-crystalline (SC) materials:

$$E_{T,SC} = \dot{M}\int_{T_1}^{T_2} C_p \times dT + \dot{M} \times H_f + \dot{M}\int_{P_1}^{P_2} \left(\frac{\partial h}{\partial P}\right)_T \times dP \quad (3)$$

For amorphous (AM) materials:

$$E_{T,AM} = \dot{M}\int_{T_1}^{T_2} C_p \times dT + \dot{M}\int_{P_1}^{P_2} \left(\frac{\partial h}{\partial P}\right)_T \times dP \quad (4)$$

where $\dot{M}$ is the mass flow rate, T_1 and T_2 are the feedstock temperatures at the input and output states respectively, P_1 and P_2 are the pressures at the input and output states respectively, C_p is the specific heat capacity of the material, H_f is the enthalpy of heat of fusion of the materials (this is zero for amorphous material), and ρ is the material density. The first and second terms of the right side of Eq. (3) are related to the energy required for melt preparation. The third term is the energy required for forming the material through the die and this is usually considered to be less than 5% of the E_T.

According to the first law of thermodynamics, the minimum energy required to go from state 1 to state 2 (see Fig. 1) can be calculated from the enthalpy changes (Δh) occur in melting (assumes that these occur at constant pressure) and forming (assumes that this occur at constant temperature) operations:

$$\Delta h = (h_2 - h_1) = \Delta h_1 + \Delta h_2 \quad (5)$$

$$\Delta h_1 = \int_{T_1}^{T_2} C_p \times dT + H_f = \overline{C}_p \times (T_2 - T_1) + H_f \quad (6)$$

$$\Delta h_2 = \int_{P_1}^{P_2} \left(\frac{\partial h}{\partial P}\right)_T \times dP = \frac{(P_2 - P_1)}{\bar{\rho}} \quad (7)$$

where h_1 and h_2 are the specific enthalpy values of the materials at the input and output states respectively, Δh_1 and Δh_2 are the enthalpy changes occur at melting and forming operations respectively, $\overline{C}_p$ is the average specific heat capacity of the polymer and $\bar{\rho}$ is the average density of the material. Then, the thermal efficiency ($\eta_{extruder,thermo}$) of an extruder is given by:

$$\eta_{extruder,thermo} = \frac{\dot{M} \times \Delta h}{E_{in}} \times 100\% \quad (8)$$

The above details describe the energy efficiency of an extruder. However, the process should be efficient in both energy and thermal terms to ensure high quality products at a low production cost. A good thermal efficiency means that the process melt out put should be uniform in temperature (i.e. the temperature uniformity of the melt over the time and across the melt flow cross-section) throughout the process operation. Moreover, the level of the melt temperature should be at the desired level and the material should have achieved the complete melting when it reaches the die. Therefore, it is better to define the overall efficiency of an extruder as a combination of both energy and thermal efficiencies.

1.2. Previous studies on thermal stability and energy consumption in polymer extrusion

Since the 1950s, numerous previous studies can be found in the literature on melting/thermal issues in polymer extrusion. However, it seems that not much attention has been paid to studies of energy related issues until the 1990s. Traditionally, polymeric materials based manufactures primarily concerned about the thermal quality of the melt which is the key to from high quality products but they did not pay much attention to process energy efficiency. As world energy prices have been gradually increasing over the last few decades, manufacturing companies start to search for methods to cut down their energy bills by making their production lines energy efficient. However, it is challenging to achieve both the required melt quality and the energy efficiency at the same time in industrial applications.

Process cooling (e.g. screw cooling, barrel cooling) is a common operation in extrusion to maintain the thermal stability of the process. Also, some amount of the process heat is naturally released to the surroundings. Therefore, a considerable portion of the supplied energy to the process is taken away by the cooling water and air [17]. In fact, it is clear that a considerable amount of the supplied energy has to be sacrificed to maintain the process thermal stability. Obviously, the process energy and thermal efficiencies are likely to be inter-related. However, there is no point of making the process more energy efficient if the melt output is not of the required thermal quality. Therefore, thermal stability and energy efficiency should be achieved consecutively. Here, the level of melt temperature fluctuations can be taken as a measure of the process thermal stability. Rasid and Wood [19] observed the die melt temperature profile and effects of barrel set temperature on extruder power consumption. They found that the metering zone set temperature has the greatest influence on the level of melt temperature while the solids conveying zone set temperature has the greatest influence on the level of extruder power consumption. Moreover, they attempted to explore the effects of melt pressure on melt temperature profile however, no significant effect was observed. No attempt was made to investigate correlation/s between extruder power and melt temperature or melting stability.

Previous work reported by Sorroche et al. [20] measured extruder energy consumption and melt temperature dynamics in parallel. They found that the extruder specific energy consumption reduced as screw speed increased despite changes to process settings and screw geometry. Melt temperature measured across an extruder output melt flow showed that the magnitude of temperature fluctuations increased with the screw speed. Such an increasing trend of thermal fluctuations may arise due to the fact that the residence time of the material reduces with the increasing speed and hence there will be less time for melting and mixing of the material.

Previous work by the author [4–7] found that the temperature across the melt flow significantly varied over the processing conditions. The magnitude of the thermal fluctuations were found to increase with screw speed. Barrel set temperature also showed some influences on melt thermal variations but to a lesser extent. Moreover, process thermal fluctuations differed depending on the screw geometry. In general, the thermal fluctuations were found to be slow in nature and these were below 0.5 Hz over the different processing situations tested (i.e. from 10 to 90 rpm over 3 different barrel set temperature conditions).

Other work by the authors [4,21] reported an attempt to predict the process thermal stability inferentially. The correlations

between the screw load torque, melt pressure and melt temperature fluctuations were examined by analysing experimentally measured signals. However, no strong correlations between these signals could be observed. It was found that as the screw load torque signal is dominated by the solids conveying torque, it was not sensitive enough to identify unstable melting issues. Pressure fluctuations had slight correlations with melt temperature fluctuations particularly at low screw speeds. However, none of these signals showed sufficiently good performance for them to be used as a tool to monitor the process thermal stability inferentially.

According to the authors' knowledge, no previous work has attempted to correlate process thermal stability and energy consumption to explore possible ways of optimising both of these parameters in parallel. Increasing both energy and thermal efficiencies may be achieved by improving the machine design, particularly by modifying screws to have better conveying, melting and mixing of the material. Also, direct drive extruders, improved heater/barrel design for reduced heat losses to the surroundings, and advanced vector control alternating current (AC) drives are some of the current topics in the extrusion field in terms of achieving an improved overall process efficiency. Ideally, for a given machine and material, thermal and energy efficiencies should be achieved through proper selection of process settings. Prior knowledge on the relationship/s between thermal and energy related parameters would therefore be invaluable.

In this work, both the extruder energy consumption and melt temperature (i.e. at the number of different radial positions across the melt flow) were observed at the same time over a number of different processing conditions. Then, these signals were used to identify any possible correlation/s between these parameters. The major aim was to identify possible ways to achieve optimal energy and thermal efficiencies at high throughput rates. A single screw extruder was used in the experiments as it is the most commonly used type in industrial polymer processing applications. Three different screw geometries and set temperature conditions were used for collecting the experimental data with single polymer material.

2. Experimental

All measurements were carried out on a highly instrumented 63.5 mm diameter (D) single screw extruder (Davis Standard BC-60) at the IRC laboratories of the University of Bradford. A gradual compression screw with 3:1 compression ratio; a tapered rapid compression screw with 3:1 compression ratio; and a barrier flighted screw with a spiral Maddock mixer and a 2.5:1 compression ratio were used to process the materials. Geometrical specifications of these screws are shown in Fig. 2.

From here onwards, these three screws are refereed as the GC screw, RC screw and BF screw, respectively. The extruder was fitted with a 38 mm diameter adapter by using a clamp ring prior to a short 6 mm diameter capillary die as shown in Fig. 3.

The extruder barrel has four separate temperature zones (each with a heater of 4 kW) and another three separate temperature zones at the clamp ring (with a heater of 0.9 kW), adapter (with a heater of 1.4 kW) and die (with a heater of 0.2 kW). All of these temperature zones are equipped with Davis Standard Dual-Therm controllers and the set temperature can be controlled individually. The extruder drive is a horizontal type separately excited direct current (SEDC) motor which has ratings: 460 Vdc, 50.0 hp (30.5 kW), at speed 1600 rpm. The motor and screw are connected through a fixed gearbox with a ratio of 13.6:1, and according to the manufacturers' information the gearbox efficiency is relatively constant at all speeds (~96%). The motor speed is controlled by a speed controller (MENTOR II) based on speed feedback obtained

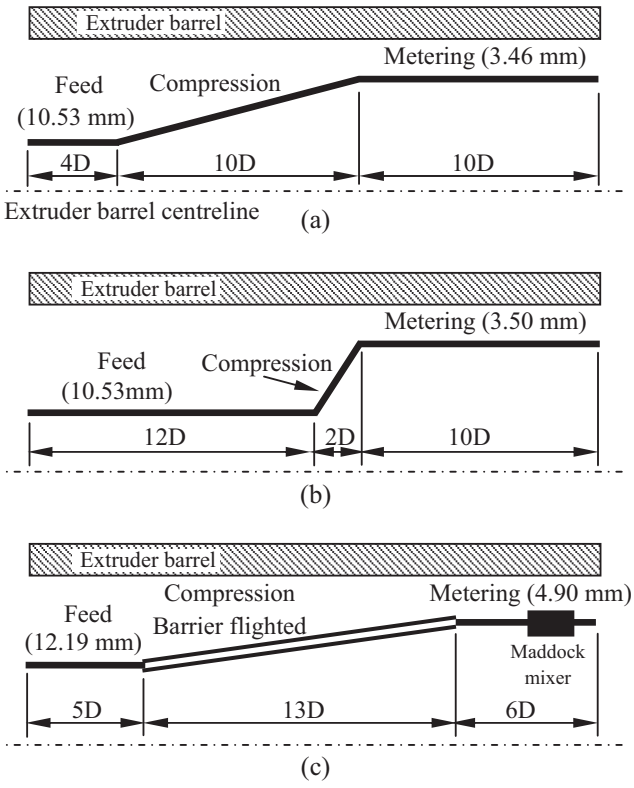

Fig. 2. Details of the screws used in experiments.

through a direct current (d.c.) tachometer generator. Moreover, cooling of the feed throat of the extruder is achieved via a water supply with a constant flow rate and also forced air cooling blowers have mounted along the extruder barrel.

Melt pressure at the adapter was recorded by a Dynisco TPT463E pressure transducer. The total extruder power and motor power were measured using a Hioki 3-phase power meter and an Acuvim IIE 3-phase power meter, respectively. Melt temperatures of the different radial locations of the melt flow at the end of the adapter (denoted as die melt temperatures throughout this paper) were measured using a thermocouple mesh placed in-between the adapter and the die as shown in Fig. 4. As it was previously confirmed by Kelly et al. [22,23], the die melt temperature measurements are symmetrical across the thermocouple mesh centreline when averaged over a significantly long period of time. Therefore, seven thermocouple junctions (distance from the melt flow centreline to each radial position (rp): Trp-0: 0 mm, Trp-2.5: 2.5 mm, Trp-5: 5 mm, Trp-8: 8 mm, Trp-11: 11 mm, Trp-14: 14 mm, Trp-16.5: 16.5 mm) were placed asymmetrically across the melt flow along the diameter of the mesh as shown in Fig. 4, and this asymmetric placement of wires gave the opportunity to increase the number of effective temperature measurements across the melt flow. Moreover, the temperature of the melt close to the die wall was measured from a flush mounted insulated wall thermocouple and this measurement was considered as the melt temperature of the 19 mm die radial position (Trp-19). Additionally, an infrared (IR) temperature sensor (Dynisco MTX 922-6/24) was used to make bulk melt temperature measurements (T-IR) of melt near the screw tip.

A data acquisition programme developed in LabVIEW was used to communicate between the experimental instruments and a PC. All signals (screw speed, melt temperature, melt pressure, power) were acquired at 10 Hz using a 16-bit DAQ card, National Instruments (NI) PCI-6035E, through a NI TC-2095 thermocouple connector box and a NI low-noise SCXI-1000 connector box.

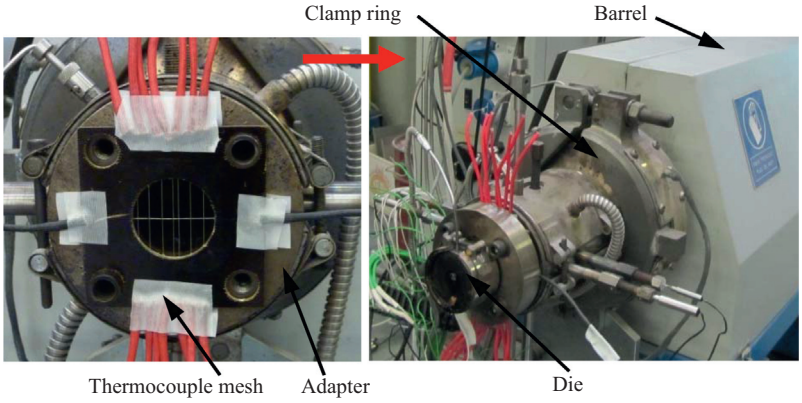

Fig. 3. Arrangement and dimensions of the apparatus.

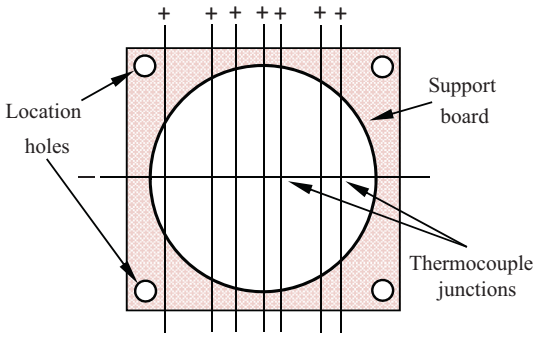

Fig. 4. The thermocouple mesh arrangement.

2.1. Materials and experimental conditions

Experimental trials were carried out on a virgin Polystyrene (PS), Styrolution PS 124N (density: 1.040 g/cm^3 and MVR: 12 cm^3/10 min). The volume melt-flow rate (MVR) and density values are presented according to the ISO 1133 (@ 200 °C, 5 kg) and ISO 1183 standards, respectively. The extruder temperature settings were fixed under three different set conditions denoted as A (low temperature), B (medium temperature) and C (high temperature) as described in Table 1.

Nine different experimental trials were carried out with the three screw geometries and three set temperature conditions, and the data was collected at 0 rpm for a small time period. Then, the screw speed was adjusted from 10 rpm to 90 rpm in steps of 20 rpm. All the data was recorded continuously whilst the extruder was allowed to stabilise at each screw speed.

3. Results and discussion

3.1. Rheological analysis of the materiel (Polystyrene)

A twin bore capillary rheometer (Rosand RH10, Malvern Instruments, UK) was used to measure the rheology of Polystyrene at extrusion process rates and temperatures. The experiments were carried out over a shear rate range of 10–1000 s^{-1} using capillary dies of 2.0 mm diameter with an entrance angle of 180°; a long die of length 32.0 mm and an orifice die with land length close to 0. Shear viscosity was calculated from measured wall shear stress at a range of shear strain rates. The Bagley ends correction [24] was applied to the results to correct for pressure loss due to convergence into the die entrance. Also the Rabinowitsch correction [25] was used for representing the pseudoplastic nature of the polymer melt. Tests were performed at three set temperatures (i.e. equivalent to the extruder set temperatures shown in Table 1):180 °C, 200 °C and 220 °C. Measured shear viscosity at each of the three set temperatures is shown in Fig. 5. The measured rheology followed temperature dependent shear thinning behaviour typical of thermoplastic polymers. The Carreau model [26,27] (which is given by Eq. (9)) was fitted to the measured rheological data at each of the set temperatures, as shown in Fig. 5. Figure legends are in the format of EXP/PRE-set temperature condition and the terms EXP and PRE are used to denote experimental and model predicted conditions, respectively.

Table 1
Extruder barrel temperature settings.

Temperature settings	Set temperatures (°C)						
	Barrel zones				Clamp ring	Adapter	Die
	1	2	3	4			
A	130	155	165	180	180	180	180
B	140	170	185	200	200	200	200
C	150	185	200	220	220	220	220

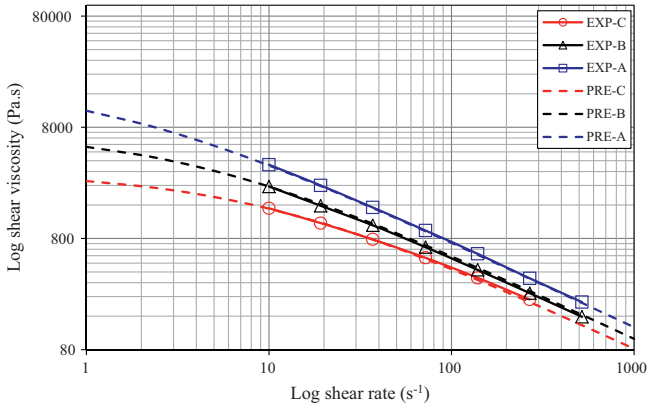

Fig. 5. Measured and predicted shear viscosity of polystyrene at set temperature conditions A, B, and C.

$$\mu(\gamma,T)=\frac{\mu_0\times f(T)}{[1+(\lambda\times\gamma\times f(T))^a]^{\frac{n-1}{a}}} \tag{9}$$

where μ is the viscosity, μ_0 is the viscosity at zero shear rate, γ is the shear rate, λ is the relaxation time, a is the shift factor, $f(T)$ is the

temperature function and n is the power law index. This model describes the shear rate dependent behaviour and is able to fit both the linear power law section of the data and predict the transformation to a Newtonian plateau at lower strain rates. Temperature dependence of the measured viscosity was modelled using the Williams–Landel–Ferry (WLF) equation [28,29] which is an empirical equation associated with time-temperature superposition and this is given in Eq. (10).

$$f(T) = \frac{C_1 \times (T_r - T_s)}{(C_2 + T_r - T_s)} - \frac{C_1 \times (T - T_s)}{(C_2 + T - T_s)} \quad (10)$$

where T_r is a reference temperature chosen to construct the compliance master curve and C_1, C_2, T_s are empirical constants adjusted to fit the values of the superposition parameter.

The purpose of modelling the measured rheological data was to enable calculation of viscosity in the channel of the extruder screw metering section at each of the experimental conditions (screw rotation speed and melt temperature). Shear strain rate at each condition was calculated from the screw rotation speed and channel depth; bulk melt temperature was determined from measurements made in the extruder die adaptor using the thermocouple mesh. Using the above models, shear viscosity at each extrusion condition was calculated, allowing specific energy consumption to be plotted against viscosity for each screw geometry and set temperature, as shown in Fig. 6.

From Fig. 6, it can be seen that specific energy consumption (SEC) ranged from 700 to over 1900 J g^{-1}. The effect of set temperature on melt viscosity was clearly observed, in general lower SEC was observed for lower melt viscosity. However there was not a direct correlation between viscosity and SEC, highlighting the complex nature of melting in polymer extrusion. Highest energy consumption was measured at low extruder screw rotation speeds; here melting is achieved primarily by conduction from the screw and barrel walls. At higher screw speeds, specific energy consumption converged to lower values between 700 and 800 J g^{-1}, due to increased levels of more efficient heating from viscous shearing. The effect of extruder geometry was also apparent, in particular the barrier flighted screw (BF) required lower specific energy than the two single flighted screws (GC and RC) at comparable viscosities. This demonstrates the more efficient melting of the barrier flighted screw for this polymer, which also incorporated a spiral mixer.

3.2. Study of the signal dynamics and correlation coefficients

The experimentally measured signals were observed for any possible correlations of their dynamics. All the signals were normalised to make it easier to observe any possible similarities of their dynamic behaviour. The normalised signals of the total extruder power, motor power, melt pressure, T-IR, Trp-0, Trp-14 and Trp-16.5 are shown in Figs. 7–9 for BF, GC and RC screws (only at set temperature condition A), respectively. From here onwards, T-IR refers to the temperature measured by the IR temperature sensor and Trp refers to the temperature of the radial position, where numbers followed by Trp are in millimeters.

As it is evident, the total power signals vary significantly over time due to the operation of the barrel heaters and cooling fans with on–off action. Otherwise, all the signals show a quite similar trend of dynamic changes with step changes in screw speed.

Correlation coefficients between each signal (under set temperature condition A) were calculated and shown in Tables 2–4 for BF, GC and RC screws, respectively. The correlation coefficient (CC) matrix is symmetric and hence only a half of the matrix is shown

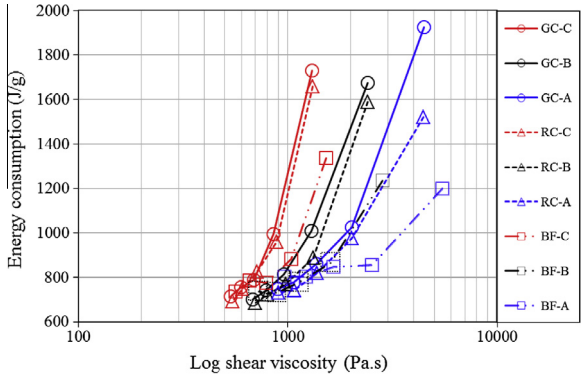

Fig. 6. Extruder specific energy consumption vs shear viscosity for Polystyrene.

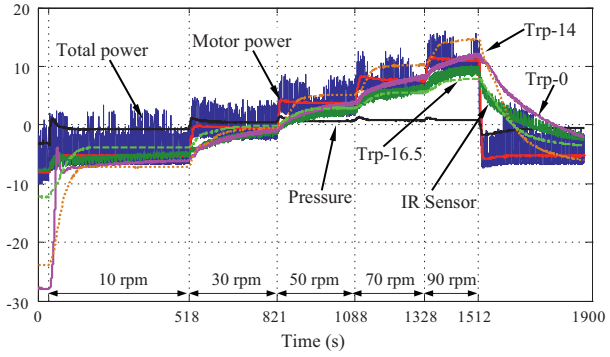

Fig. 7. The normalised process signals measured with the BF screw at set temperature condition A.

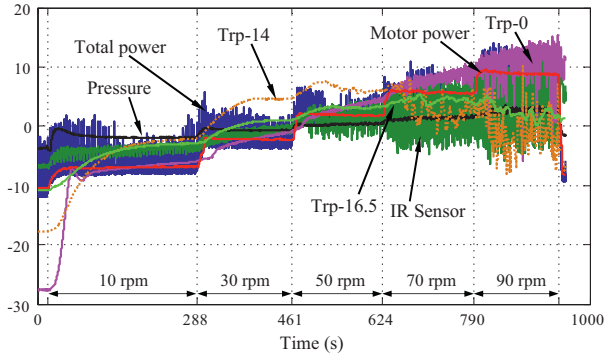

Fig. 8. The normalised process signals measured with the GC screw at set temperature condition A.

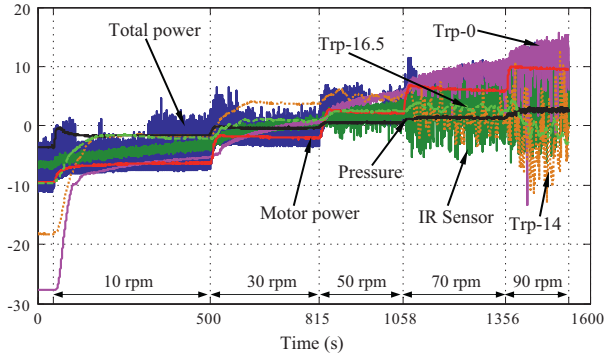

Fig. 9. The normalised process signals measured with the RC screw at set temperature condition A.

Table 2
Correlation coefficients between each of the individual signals for the BF screw at set temperature condition A.

	T-Power	M-Power	T-IR	Pressure	Trp-0	Trp-14	Trp-16.5
T-Power	1.000						
M-Power	**0.949**	1.000					
T-IR	**0.812**	**0.850**	1.00				
Pressure	0.773	**0.817**	0.569	1.000			
Trp-0	0.670	0.702	**0.902**	0.558	1.000		
Trp-14	**0.800**	**0.846**	**0.944**	0.639	**0.945**	1.000	
Trp-16.5	0.799	**0.846**	**0.944**	0.636	**0.936**	**0.999**	1.000

Table 3
Correlation coefficients between each of the individual signals for the GC screw at set temperature condition A.

	T-Power	M-Power	T-IR	Pressure	Trp-0	Trp-14	Trp-16.5
T-Power	1.000						
M-Power	**0.962**	1.000					
T-IR	0.732	0.771	1.00				
Pressure	**0.942**	**0.973**	0.762	1.000			
Trp-0	**0.842**	**0.894**	0.761	**0.873**	1.000		
Trp-14	0.496	0.540	0.453	0.446	0.650	1.000	
Trp-16.5	0.797	**0.848**	0.708	0.777	**0.902**	**0.845**	1.000

Table 4
Correlation coefficients between each of the individual signals for the RC screw at set temperature condition A.

	T-Power	M-Power	T-IR	Pressure	Trp-0	Trp-14	Trp-16.5
T-Power	1.000						
M-Power	**0.963**	1.000					
T-IR	**0.833**	**0.867**	1.00				
Pressure	**0.944**	**0.974**	**0.852**	1.000			
Trp-0	**0.862**	**0.904**	**0.818**	**0.900**	1.000		
Trp-14	0.379	0.418	0.431	0.429	0.663	1.000	
Trp-16.5	0.641	0.690	0.633	0.668	**0.850**	**0.837**	1.000

in the tables. Correlation coefficients higher than 0.8 are shown in bold. Normally, correlation coefficient represents the normalised measure of the strengths and directions of the linear relationship between two variables and this ranges from −1 to 1, where positive values indicate that variables are positively correlated (i.e. variables vary in the same direction) and the strength of the positive correlation increases from 0 to 1. Negative values specify that variables are negatively correlated (i.e. variables vary in the opposite directions) while the strength of the negative correlation between signals increases from 0 to −1. Values close to or equal to 0 suggest there is no linear relationship between the variables.

As was expected, total extruder power and motor power signals show strong correlations with all the screws used. Correlations between the total power and melt pressure are also strong for GC and RC screws (i.e. CC is around 0.94) while it is less strong with the BF screw as well (i.e. CC is around 0.77). Correlations between motor power and melt pressure are stronger than the pressure-total power correlations for all the screws. Correlations between power and melt temperature signals differed depending on the screw geometry. Of the four melt temperature signals, T-IR, Trp-0 and Trp-0 show the highest correlations with the total extruder power or motor power for BF, GC, and RF screws, respectively. Total and motor power signals relating to the GC and RC screws show good correlations with melt temperature signal measured at the middle of the flow (i.e. Trp-0) while these signals relating to the BF screw indicate good correlations with the melt temperature measurements close to the die wall than the middle of the flow.

3.3. Comparison of the power and melt temperature signals

Data collected over the last minute at each screw speed (i.e. after process became stable) were used for plotting the graphs presented in this section and most of the sub-graphs are plotted in the same scale for the ease of comparison.

The average values of the total extruder power (TP), fluctuations of the total extruder power (ΔTP), motor power (MP), fluctuations of the motor power (ΔMP) and the difference between the total power and the motor power (TP–MP) at each screw speed are shown in Fig. 10.

As it is evident, the total extruder power increased with the screw speed quite linearly for all the screws while the power fluctuations increased with increase in barrel set temperature regardless the screw geometry. However, these is no clear link between the total power fluctuations and the screw speed. The motor power also increased linearly with screw speed for all screws but motor power fluctuations are significantly lower compared to the total power variations. Therefore, the majority of variations induced into the total power signal may be due to the on–off action of the barrel heaters and cooling fans of the extruder.

Usually, the difference between the total and motor power signals is the power consumed by the process heating/cooling system, control electronics and other auxiliary equipment. In this study, no auxiliary equipment was employed and hence these values show the power consumed by the process heating/cooling system only (as the typical power consumption of the control electronics is very low at approx. 0.35 kW). Screw speeds corresponding to the highest to lowest value of TP–MP at each set temperature condition for different screws are shown in Table 5.

As it is evident, the heating/cooling system has demanded the highest power at 10 rpm under the set temperature conditions A and B where it is at the 30 rpm for set temperature condition C. Conversely, power demand of the heating/cooling system has gradually reduced in the order of 10–90 rpm at set temperature condition B regardless the screw geometry but this is not true at

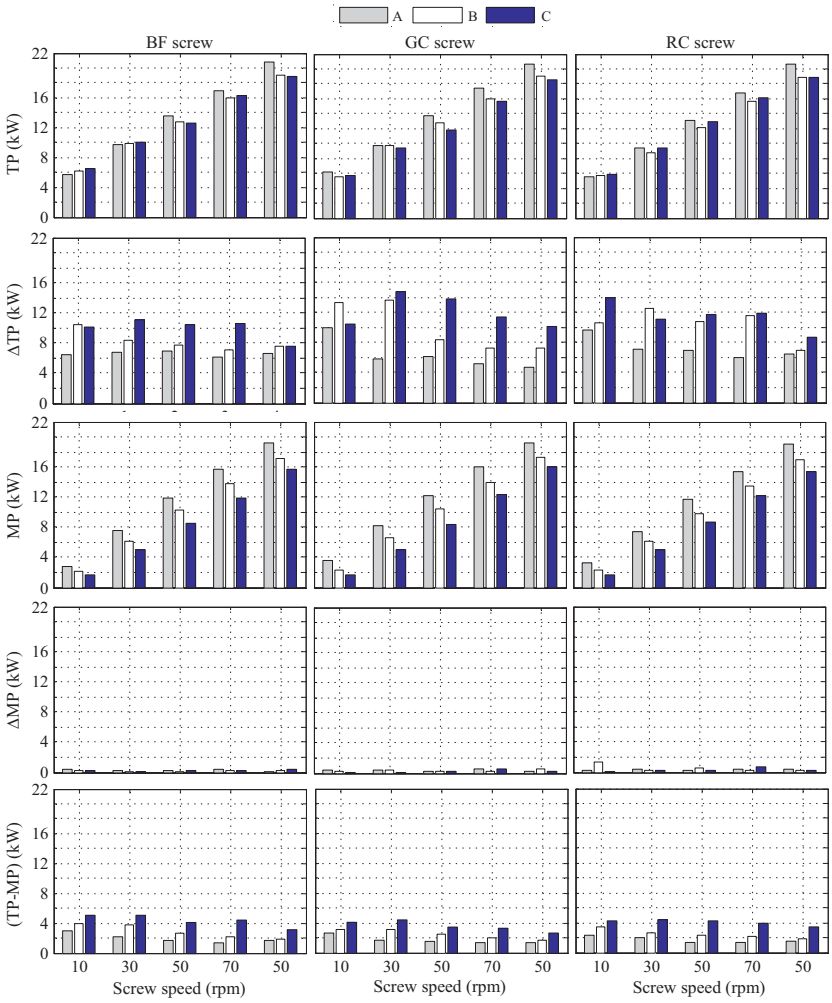

Fig. 10. Details of the process energy demand over different processing conditions and screws.

Table 5
The screw speeds corresponding to the highest to lowest value of TP–MP at each set temperature condition.

Screw	Corresponding screw speeds in descending order of TP–MP														
	A					B					C				
BF	10	30	50	90	70	10	30	50	70	90	30	10	70	50	90
GC	10	30	50	90	70	10	30	50	70	90	30	10	50	70	90
RC	10	30	90	50	70	10	30	50	70	90	30	50	10	70	90

conditions A and C. Such complex differences of power demand may occur due to the variations of material viscosity, amount of mechanical heat generation, frictional properties of the materials, etc., which may happen with the barrel set temperature changes. An experiment carried out by Cantor [30] with three different materials and screw geometries observed that the difference between the total extruder power and motor power reduces with the screw speed with all the materials and screw geometries tested. However, this experiment was conducted with only a single barrel set temperature condition.

As shown in Fig. 10, the difference between the total and motor power signals increased with the increase of the barrel set temperature with all the screws. Actually, this increase of power demand by the heating/cooling system is quite obvious with the increase of barrel set temperatures. Conversely, it is well-known that the heat generated by the process mechanical work increases with the screw speed. Therefore, it can be argued that the amount of heat input by the heating system should reduce as screw speed increased as the heat generated by the screw mechanical work increases, to maintain the process thermal stability. However, experimental results show that the power demand of the heating/cooling system is not always reduced with the increasing screw speed and depend on the level of set temperature and screw geometry as shown in Table 5. This highlights the complex nature of process energy consumption in polymer extrusion.

The mass throughput, specific energy consumption of the extruder (SEC-Extruder) and the specific energy consumption of the motor (SEC-Motor) at each speed (i.e. average values) are shown in Fig. 11.

Mass throughput increases with screw speed as expected and slight differences in the rate can be observed with the barrel set temperature and screw geometry at the same screw speed. Also, it is noticeable that the SEC values of the extruder at 10 rpm (where conductive heat is the dominant) are considerably higher

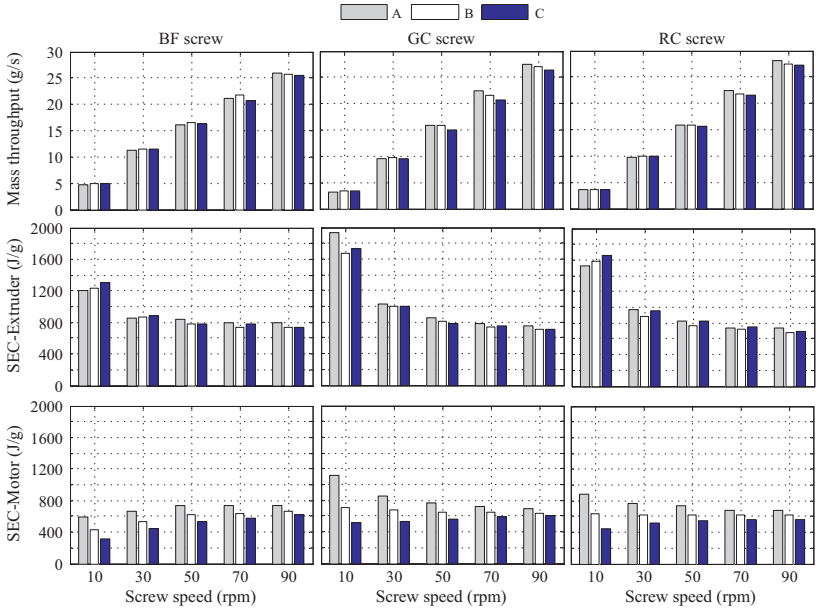

Fig. 11. Process mass throughput and SEC of the extruder/motor over different processing conditions.

than other speeds with all screws. Moreover, it is clear that SEC of the extruder reduces with increase of screw speed regardless of the differences in the screw geometry and barrel set temperatures. However, the SEC of the motor does not reduce with screw speed and shows an increasing trend with screw speed at all set temperature conditions with the BF screw and at the set temperature condition C with the GC and RC screws. Conversely, the SEC of the motor is similar at all screw speeds at the set temperature condition B with the GC and RC screws. A similar trend to this study was observed for the SEC of an extruder with the same BF, GC and RC screws by Kelly et al. [22] for a low density polyethylene (LDPE). Moreover, they observed a reducing trend of the SEC of the motor as well for all the screws with this LDPE. Therefore, it clear that the nature of the motor SEC may depend on the material type, screw geometry and set temperature condition.

The mean temperature across the melt flow (i.e. the average of the mean temperature values at the different radial positions: 0 mm, 2.5 mm, 5 mm, 8 mm, 11 mm, 14 mm, 16.5 mm and 19 mm), the difference between the maximum (i.e. the average of the maximum values of different radial positions) and minimum (i.e. the average of the minimum values of different radial positions) temperatures across the melt flow (ΔT) and the difference between the maximum and minimum melt pressures (ΔP) were calculated and these details are shown in Fig. 12.

These figures clearly indicate that the melt temperature fluctuations increase with screw speed (regardless of the screw geometry) although the SEC of the extruder shows a reducing trend with increasing screw speed. As process speed increases, material has less time inside the barrel prior to entering to the die. Since polymers are poor thermal conductors there may not be enough time for good melting and mixing to occur and give a uniform melt at high speeds and this may cause an increase of thermal fluctuations at increasing process speeds. Moreover, the results show that these thermal variations are dependent upon the die radial

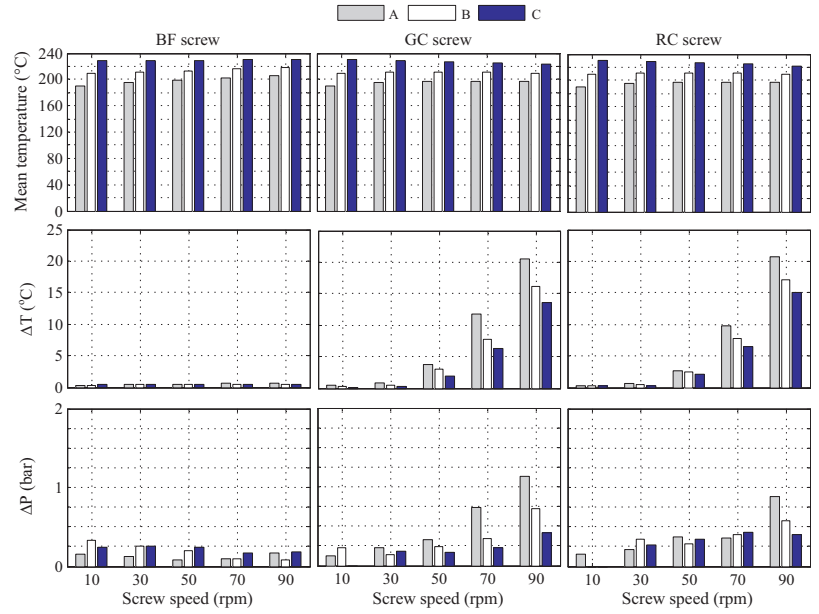

Fig. 12. Mean melt temperature across the melt flow, ΔT and ΔP over different processing conditions and screws.

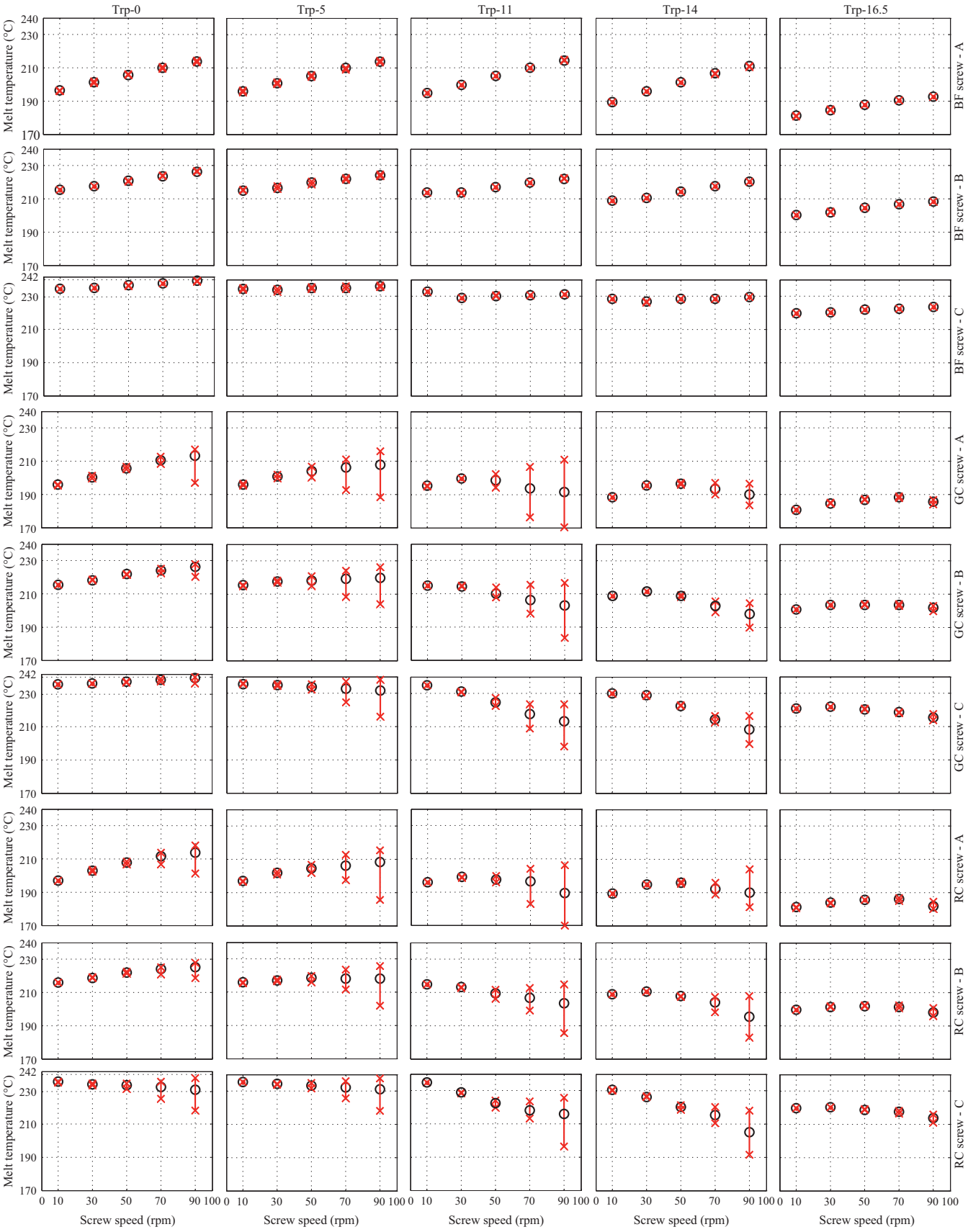

Fig. 13. Mean melt temperature observed at each radial position together with the magnitude of fluctuations.

position and screw geometry as well. With GC and RC screws, melt temperature fluctuations are reduced with increase of the barrel set temperature which is the opposite trend to the total extruder power fluctuations. With the BF screw, thermal fluctuations do not show a clear trend (however fluctuations are very low compared to other two screws) with an increase of the barrel set temperatures while total power fluctuations show an increasing trend. The BF screw shows the lowest thermal fluctuations among the three screws. Therefore, it can be argued that the specific design of the BF screw with solid melt separation and Maddox mixer leads to improved melting/mixing performance of the material. Furthermore, the SEC of the extruder is relatively low with the BF screw compared to the GC and BF screws. Generally, it seems that the BF screw has better thermal and energy efficiency than the other two screws in processing of this particular material. Some of the previous work also reported that the BF screws perform favourably (e.g. efficient melting and mixing) compared to conventional single-flighted screws [22,31].

To obtain an extensive understanding of the thermal behaviour across the melt flow cross-section, the mean melt temperatures across the melt flow at each radial position were calculated together with the magnitude of fluctuations (i.e. the difference between the lowest and the highest melt temperatures values) for all the screw geometries at each screw speed and set temperature condition. The corresponding details relevant to the temperature measurements Trp-0, Trp-5, Trp-11, Trp-14 and Trp-16.5 are shown in Fig. 13. All the sub-figures are shown in the same scale and hence a comparison can be made on the melt temperature variations at different processing conditions.

It is clear that melt temperature fluctuations are considerably lower with the BF screw than the GC and RC screws regardless the radial position, processing speed and the barrel set temperature. In general, the mean melt temperature increases with screw speed at the middle of the melt flow (i.e. at the Trp-0) with all the screws but this is not true with the other radial positions across the melt flow. In comparing power and melt temperature behaviours, it is clear that:

- In general, power variations reduce with the screw speed where melt temperature variations show an increasing trend.
- Power variations increase with the increase of barrel set temperature where melt temperature variations show a reducing trend.
- Process energy demand (i.e. the levels of the both total and motor power signals) increases with the screw speed but the melt temperature of some of the radial positions does not increase with the screw speed.
- Changes to the level of mean power demand are quite linear with screw speed but melt temperature shows a non-linear behaviour and this depends on the die radial position, screw geometry and barrel set temperature conditions as well.

Generally, it is clear that the relationship/s between thermal fluctuations and energy consumption differs depending on the screw speed and set temperature conditions, and these are likely to be dependent upon material properties as well (polymer viscosity is dependent on shear stress which in turn depends on the screw configuration. Different polymers will display different rheological responses at a particular shear stress). Therefore, it is better to conduct more research in this area to investigate further about the possible relationship/s between process thermal stability and energy efficiency.

3.4. Modelling of total power demand

Eventually, an attempt was made to identify the relationship between the mean total power (TP), screw speed (ω_{sc}), mean temperature across the melt flow (T_{mean}) and the level of the melt temperature fluctuations across the melt flow (ΔT). Here, the TP relating to all experiential conditions used in this study was modelled as a function of the other variables based on the modelling technique discussed previously [5,7–9,32]:

$$TP = f(\omega_{sc}, T_{mean}, \Delta T) \tag{11}$$

Of the model examined, a 3rd order model with 5 terms (which shows a root mean square error of 0.1 on an unseen data) which is given in Eq. (12) was selected for the discussion.

$$TP = 1.7981 \times \omega_{sc} + 0.0197 \times T_{mean} - 0.0143 \times \omega_{sc} \times T_{mean} + 3.1224 \times 10^{-5} \times \omega_{sc} \times T_{mean}^2 - 0.0424 \times \Delta T \tag{12}$$

A comparison of the experimental and model predicted mean total power at different speeds is shown in Fig. 14.

Evidently, there is a good fit between the experimental measurements and model predictions. This type of model may be useful for optimising a particular machine/material combination for thermal and energy efficiency, and it will be considered under future work.

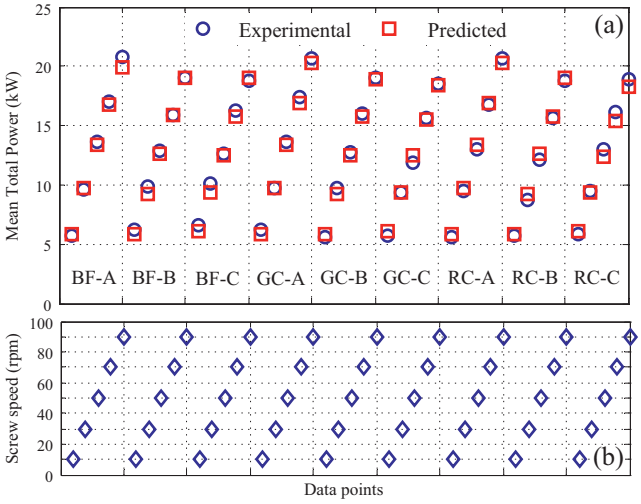

Fig. 14. (a) Experimental and model predicted mean total power at different speeds. (b) The corresponding screw speeds.

4. Conclusions

This study aimed to explore strategies for determining an optimum process operating point by optimising both the extruder energy and thermal efficiency. An attempt was made to investigate the possible correlation/s between melt temperature stability/fluctuations and energy consumption in polymer extrusion. The results showed that the SEC of the extruder reduces with the screw speed regardless the screw geometry. However, the SEC of the motor was shown to increase with screw speed for a BF screw while it reduced with screw speed for GC and RC screws. Generally, process energy efficiency increases with screw speed. However, process thermal fluctuations increase with screw speed and these variations depend on the screw geometry and the die radial position as well. Conversely, melt temperature shows an increasing trend with screw speed only at the middle of the flow while an opposite trend can be observed at other radial locations away from the melt flow centre. Correlation/s between the thermal stability and energy efficiency are highly complex and dependent upon all machine, material and process parameters. According to the results of this work, it is difficult to achieve the energy efficiency achievable at high

running speeds without increasing thermal fluctuations and thus reducing thermal efficiency. Further research is highly recommended in this area to determine an accurate generalised model relating process thermal stability, energy efficiency and all other relevant parameters which will allow selection of an optimum operating point for a given machine and material.

Acknowledgments

This work was funded through an inter-disciplinary research programme (Grant No. EP/G059330/1) by the EPSRC-UK. The technical assistance provided by Ken Howell, Roy Dixon and John Wyborn is greatly appreciated.

References

[1] Rosato DV, Schott NR, Rosato DV, Rosato MG. Plastics engineering, manufacturing & data handbook: fundamental and processes, vol. 2. Kluwer Academic Publishers; 2001. p. 54–65.
[2] Abeykoon C, McAfee M, Thompson S, Li K, Kelly AL, Brown EC. Investigation of torque fluctuations in extrusion through monitoring of motor variables. In: Proceedings of 26th PPS annual Europe/Africa regional meeting, Larnaca, Cyprus. Paper no: 22-O.
[3] Abeykoon C, McAfee M, Li K, Martin PJ, Deng J, Kelly AL. Modelling the effects of operating conditions on motor power consumption in single screw extrusion. In: Proceedings of LSMS 2010 and ICSEE 2010 6329, vol. 2; 2010. p. 9–20.
[4] Abeykoon C, McAfee M, Li K, Kelly AL, Brown EC. Monitoring the effect of operating conditions on melt temperature homogeneity in single-screw extrusion. In: SPE ANTEC technical papers; 2010. p. 1799–806.
[5] Abeykoon C, Li K, McAfee M, Martin PJ, Niu Q, Kelly AL, et al. A new model based approach for the prediction and optimisation of thermal homogeneity in single screw extrusion. Control Eng Pract 2011;19(8):862–74.
[6] Abeykoon C, Martin PJ, Kelly AL, Brown EC. A review and evaluation of melt temperature sensors for polymer extrusion. Sens Actuat A: Phys 2012;182:16–27.
[7] Abeykoon C. Modelling and control of melt temperature in polymer extrusion. Ph.D. thesis. United Kingdom: Queen's University Belfast; 2011.
[8] Abeykoon C. A novel soft sensor for real-time monitoring of die melt temperature profile in polymer extrusion. IEEE Trans Ind Electron. http://dx.doi.org/10.1109/TIE.2014.2321345.
[9] Abeykoon C. A novel model-based controller for polymer extrusion. EEE Trans Fuzzy Syst. http://dx.doi.org/10.1109/TFUZZ.2013.2293348.
[10] Burmann G, Fischer P, Michels R. High-tech extrusion with barrier-mixing screws and spiral mandrel extrusion dies. In: Proceeding of conference on advances in plastics technology, Katowice, Poland.
[11] Rosato DV. Extruding plastics – a practical processing handbook. Springer: Verlag; 1998.
[12] Spalding MA, Hyun KS. Troubleshooting mixing problems in single-screw extruders. SPE ANTEC technical papers vol. 1; 2003. p. 229–233.
[13] Rauwendaal C. Polymer extrusion. 4th ed. Hanser; 2001.
[14] Abeykoon C. Polymer extrusion: a study on thermal monitoring techniques and melting issues. Lap Lambert Academic Publishing: Verlag; 2012.
[15] Wahla PR, Trefferb D, Mohra S, Roblegga E, Koschera G, Khinast JG. Inline monitoring and a PAT strategy for pharmaceutical hot melt extrusion. Int J Pharm 2013;455(1–2):159–68.
[16] Saerens L, Vervaet C, Remon JP, Beer TD. Process monitoring and visualization solutions for hot-melt extrusion: a review. J Pharm Pharmacol 2014;66(2):180–203.
[17] Drury B. The control techniques drives and controls handbook. London (UK): The Institution of Electrical Engineers; 2010. p 308–12.
[18] Vlachopoulos J, Strutt D. Overview: polymer processing. Mater Sci Technol 2003;19:1161–9.
[19] Rasid R, Wood AK. Effect of process variables on melt temperature profiles in extrusion process using single screw plastics extruder. Plast Rubb Compos 2003;32(5):193–8.
[20] Sorroche JV, Kelly AL, Brown EC, Coates PD, Karnachi N, Harkin-Jones E, et al. Thermal optimisation of polymer extrusion using in-process monitoring techniques. Appl Therm Eng 2012;53(2):405–13.
[21] Abeykoon C, McAfee M, Li K, Martin PJ, Kelly AL. The inferential monitoring of screw load torque to predict process fluctuations in polymer extrusion. J Mater Process Technol 2011;211(12):1907–18.
[22] Kelly AL, Brown EC, Coates PD. The effect of screw geometry on melt temperature profile in single screw extrusion. Polym Eng Sci 2006;46(12):1706–14.
[23] Brown EC, Kelly AL, Coates PD. Melt temperature field measurement in single screw extrusion using thermocouple meshes. Rev Sci Instrum 2004;75(11):4742–8.
[24] Bagley EB. End corrections in capillary flow of polyethylene. J Appl Phys 1957;28(5):624–7.
[25] Bird RB, Armstrong RC, Hassager O. Dynamics of polymeric liquids. Fluid mechanics, 2nd ed., vol. 1. New York: Wiley; 1987.
[26] Carreau PJ. Rheological equations from molecular network theories. Ph.D. thesis. Madison (USA): University of Wisconsin; 1968.
[27] Carreau PJ. Rheological equations from molecular network theories. Trans Soc Rheol 1972;16(1):99–127.
[28] Ferry JD, Landel RF, Williams ML. Extensions of rouse theory of viscoelastic properties to undiluted linear polymers. J Appl Phys 1995;26(4):359–62.
[29] Helleloid GT. On the computation of viscosity-shear rate temperature master curves for polymeric liquids. Morehead Electron J Appl Math 2001;1(1):1–11.
[30] Cantor KM. Analyzing extruder energy consumption. SPE ANTEC technical papers, vol. 2; 2010. p. 1300–6.
[31] Brown EC, Kelly AL, Coates PD. Melt temperature homogeneity in single screw extrusion: effect of material type and screw geometry. SPE ANTEC technical papers; 2004. p. 183–7.
[32] Abeykoon C, Martin PJ, Li K, Kelly AL. Dynamic modelling of die melt temperature profile in polymer extrusion: effects of process settings, screw geometry and material. J Appl Math Model 2014;28(4):1224–36.